ELSEVIER

Journal of Alloys and Compounds 431 (2007) 287–291

Journal of ALLOYS AND COMPOUNDS

www.elsevier.com/locate/jallcom

Structural and optical properties of nanostructured TiO_2 thin films fabricated by glancing angle deposition

Sumei Wang [a,b], Guodong Xia [a,b,*], Hongbo He [a], Kui Yi [a], Jianda Shao [a], Zhengxiu Fan [a]

[a] *Shanghai Institute of Optics and Fine Mechanics, Chinese Academy of Sciences, P.O. Box 800-211, Shanghai 201800, PR China*

[b] *Graduate School of the Chinese Academy of Sciences, PR China*

Received 22 February 2006; received in revised form 8 May 2006; accepted 16 May 2006
Available online 23 June 2006

Abstract

TiO_2 films deposited by electron beam evaporation with glancing angle deposition (GLAD) technique were reported. The influence of flux angle on the surface morphology and the microstructure was investigated by scanning electron microscopy. The GLAD TiO_2 films are anisotropy with highly orientated nanostructure of the slanted columns. With the increase of flux angle, refractive index and packing density decrease. This is caused by the shadowing effect dominating film growth. The anisotropic structure of TiO_2 films results in optical birefringence, which reaches its maximum at the flux angle $\alpha = 65^\circ$. The maximum birefringence of GLAD TiO_2 films is higher than that of common bulk materials. It is suggested that glancing angle deposition may offer an effective method to obtain tailorable refractive index and birefringence in a large continuous range.

Keywords: Thin films; Vapor deposition; Microstructure; Optical properties; Scanning electron microscopy

1. Introduction

Recently, glancing angle deposition (GLAD) technique has attracted considerable attention for designing the morphology of the nanostructured films [1,2]. This technique employs substrate inclination and substrate rotation, which were driven by two-step motors controlled by a computerized program [3,4]. GLAD technique has been shown to be capable of producing films with various microstructures, such as vertical columns [5], helix [6], which is hardly obtained from the normal incidence vapor deposition. Many important physical and chemical properties of thin films are determined by the microstructure and texture directly. For instance, films with a dendritic structure have been shown to work well in solar cell applications [7], whereas porous structures are used as gas sensors [8] and photocatalysts [9]. Thus, many novel physical and chemical properties of thin films can also be easily engineered.

Titanium dioxide (TiO_2) has gained extensive interest for its important role in many applications, such as catalyst, photocatalyst [9], gas sensor [8], and optical and optoelectrical [10] devices. Especially, TiO_2 thin films are useful for optical devices due to their desirable properties such as high refractive index, low absorption coefficient and high transparency in the visible and near-infrared region [11]. In the present paper, nanostructured TiO_2 thin films grown by glancing angle deposition technique are studied. The film microstructure and morphology are analyzed by cross-sectional and surface SEM images. The effect of flux angle on the structure and optical properties was investigated. The birefringence property induced by anisotropic structure was also discussed.

2. Experimental details

TiO_2 thin films were deposited by electron beam evaporation with glancing angle deposition technique. BK7 glass (Ø 30 mm × 3 mm) and n-Si(1 0 0) substrates were ultrasonically cleaned in acetone and ethanol before introduced into the vacuum system. The distance between evaporation sources and substrate was 27 cm. The background pressure was less than 2.0×10^{-3} Pa. To promote formation of stoichmetric TiO_2 films at the substrates, O_2(g) was introduced into the chamber at a flow rate such that the pressure during the deposition was

* Corresponding author. Tel.: +86 021 69918476.
E-mail addresses: wangsumei3000@163.com (S. Wang), xiaguodong2007@hotmail.com (G. Xia).

0925-8388/$ – see front matter © 2006 Elsevier B.V. All rights reserved.
doi:10.1016/j.jallcom.2006.05.091

2.3×10^{-2} Pa. Flux incident angle, defined as the angle between the incident flux and substrate surface normal, was fixed to be $\alpha = 0^\circ, 20^\circ, 40^\circ, 60^\circ, 65^\circ, 70^\circ, 75^\circ$ and 80° without substrate rotation. During deposition process, the substrate was kept at room temperature.

The surface and cross-sectional morphology was observed by field emission scanning electron microscopy (SEM) in HITACHI S-4700 microscope. In preparation for SEM observation, the films were coated with a thin layer of gold.

Transmittance spectra were measured by Lambda 900 spectrophotometer (Perkin-Elmer Company). The measurement accuracy of the equipment was ±0.08%. The effective refractive index was calculated by Swanepoel's method [12,13]. For the films with weak absorption, the transmission T can be viewed as a functions of λ:

$$T = \frac{16 n_0 n_s n_f^2 \alpha}{C_1^2 + C_2^2 \alpha^2 + 2 C_1 C_2 \alpha \cos(4\pi n_f d/\lambda)}$$

where $C_1 = (n_0 + n_f)(n_f + n_s)$, $C_2 = (n_0 - n_f)(n_f - n_s)$ and $\alpha = \exp(-4\pi k d/\lambda)$. And n_0, n_s, n_f are refractive indices of air, substrate and thin films, respectively. In the case of $n_f > n_s$,

$$T_{max} = \frac{16 n_0 n_s n_f^2 \alpha}{(C_1 + C_2 \alpha)^2},$$

$$T_{min} = \frac{16 n_0 n_s n_f^2 \alpha}{(C_1 - C_2 \alpha)^2}$$

T_{max} and T_{min} are considered to be continuous functions of λ and n_f. These functions are envelops of the maxima and minima in the transmission spectrum. Then n_f can be determined from n_0, n_s, T_{max} and T_{min} at the same wavelength:

$$n_f = \sqrt{N \pm \sqrt{N^2 - n_0^2 n_s^2}}$$

where

$$2N = n_0^2 + n_s^2 + 4 n_0 n_s \left(\frac{1}{T_{min}} - \frac{1}{T_{max}} \right)$$

3. Results and discussion

The typical cross-sectional morphologies of TiO_2 films deposited at 60–80° are shown in Fig. 1. GLAD TiO_2 films exhibit a slanted column growth. The intercolumnar pore is opened and increases with the increase of flux angle. The films are mixture of slanted columnar structure and pores. As flux angle changes from 60° to 80°, the columns become increasingly separated and distinguishable. The mean diameter of each column grows larger, from about 30 to 50 nm. These cross-sectional morphologies are in agreement with the zone 1 structure of Thornton's structural zone model [14], which is caused by the limited mobility of the incoming atoms during obliquely deposition [15].

It can be seen that the columns incline towards the direction of the incoming flux. The higher the flux angle is, the greater the column inclination is. The highly orientated nanostructure of the slanted columns indicates that GLAD TiO_2 films are anisotropy [16], with the long axis parallel to the columnar growth direction. The anisotropic structure will introduce the anisotropic dependence into the thermal, electrical, magnetic and optical properties of thin films [17]. The bundling behavior of the slanted

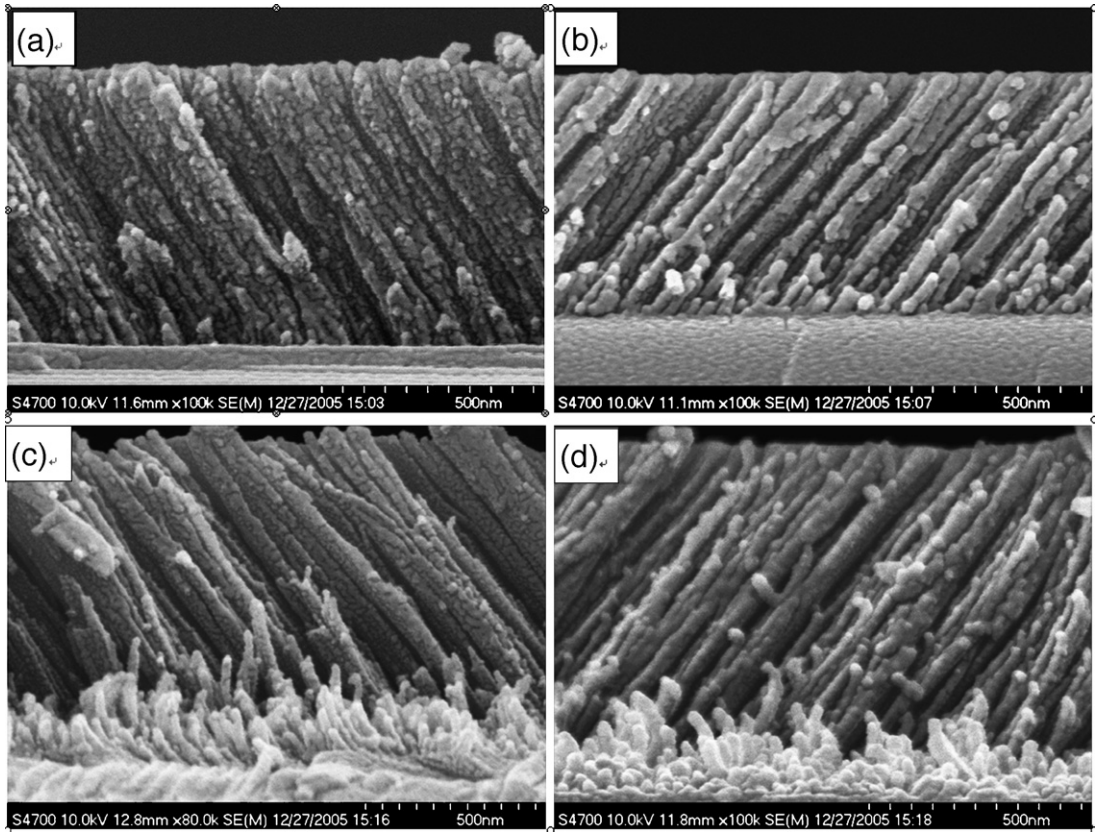

Fig. 1. Cross-sectional SEM images of the TiO_2 films deposited at different flux angles. (a) $\alpha = 60^\circ$; (b) $\alpha = 70^\circ$; (c) $\alpha = 75^\circ$; (d) $\alpha = 80^\circ$.

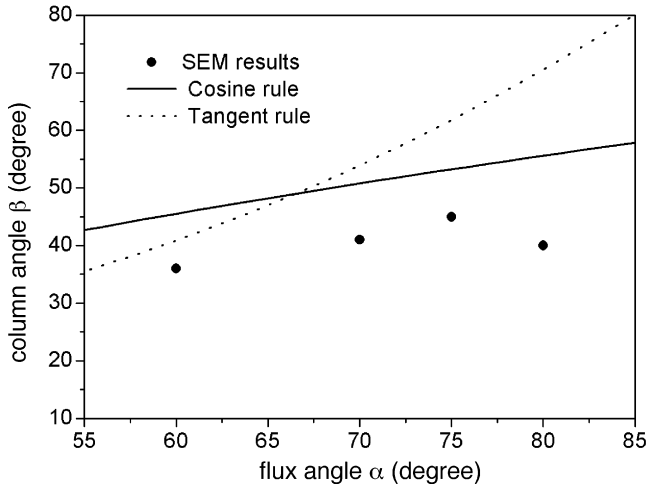

Fig. 2. The experimental and estimated column angles at different flux angles.

columns is observed at higher flux angle of GLAD TiO_2 films, which is the result of anisotropic shadowing effect [18].

Column angle β, defined as the angle between substrate surface normal and the long axis of slanted columns, is a significant structural parameter. As can be seen, the column angle increases with the increase of flux angle. The experimental and estimated column angles with different flux angles are illustrated in Fig. 2. An empirical formula known as tangent rule [19] has been developed to estimate column angle at oblique incidence: $\tan\beta = 0.5\tan\alpha$. The experimental column angle measured from SEM images is about 36° at $\alpha = 60°$, which is fairly close to the value estimated by the tangent rule. However, the difference between the experimental and estimated values grow larger for $\alpha > 70°$, as shown in Fig. 2. Another formula known as cosine rule [20], $2\sin(\alpha - \beta) = 1 - \cos\alpha$, can be much more successful in estimating the column angle of thin films deposited at highly oblique angles ($\alpha > 70°$).

It should be noted that the measured column angle deviates slightly from the empirical formula. In other words, the direction of the column growth is still nearer to the substrate normal. The same trend was also found in obliquely deposited ZrO_2 films, which exhibited even finer morphological features [15]. The origin of that deviation is the great surface curvature of nanostructured films grown by glancing angle deposition. This will distinctly change the direction of column growth compared to that of micro-sized thin films.

The porous structure of GLAD TiO_2 films can also be observed in top view SEM images, as shown in Fig. 3. At $\alpha = 60°$, the pore in the slanted columns is very small, and the film is relatively dense. At $\alpha = 75°$ and 80°, there are a great deal of pores in the neighboring columns. Characteristic of GLAD technique is the enhanced shadowing effect and limited atom diffusion during film growth [21]. The shadowing effect dominates the grow process of GLAD film, thus a porous and low-density thin

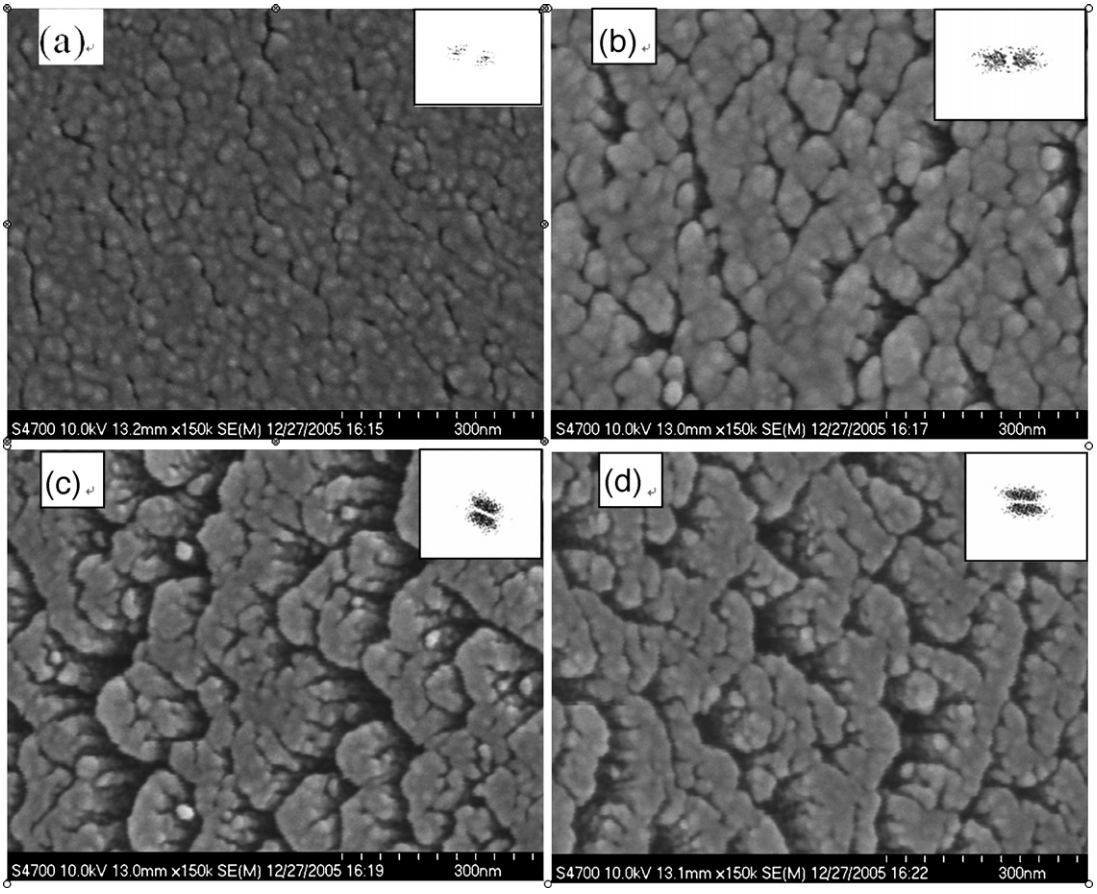

Fig. 3. The top view SEM images of GLAD TiO_2 films. (a) $\alpha = 60°$; (b) $\alpha = 70°$; (c) $\alpha = 75°$; (d) $\alpha = 80°$. Inset is a two dimensional FFT of the corresponding surface images.

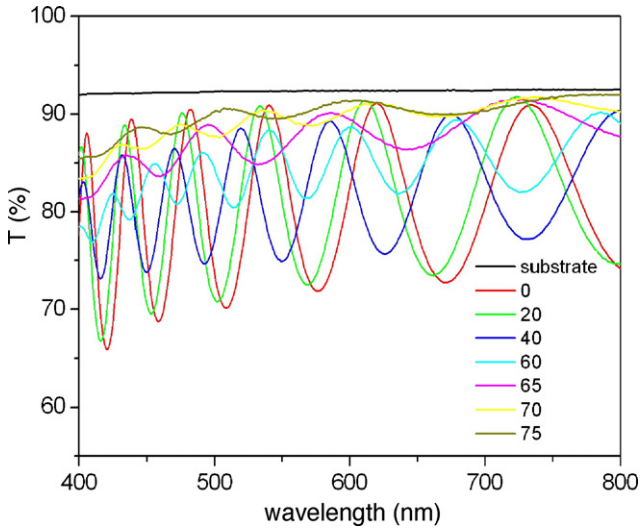

Fig. 4. Transmittance spectra of GLAD TiO_2 films deposited at different incident angles.

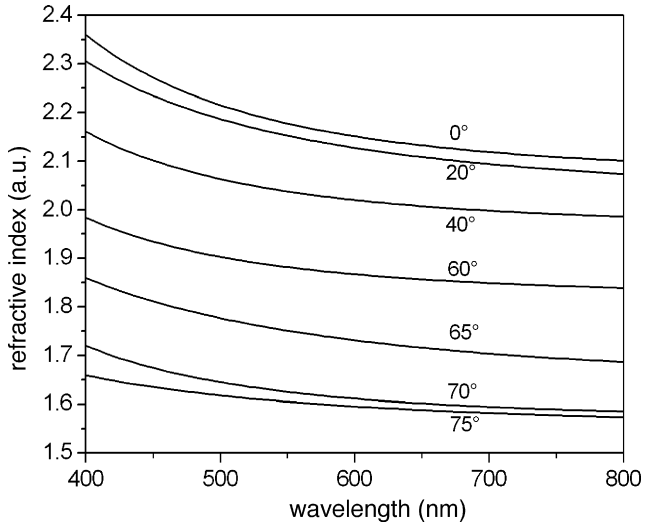

Fig. 5. Refractive indices disperse curves of GLAD TiO_2 films deposited at different incident angles.

films were produced. Greater flux angle leads to larger column angles, larger separations between neighboring columns, and higher porosity of thin films.

The anisotropic structure of slanted columns can be illustrated in a fast Fourier transform (FFT) inset in Fig. 3. The Fourier transform is represented by its amplitude spectrum, which is a plot of the absolute values of the complex Fourier components. A structure lacking in-plane anisotropy yields a circularly symmetric FFT image, whereas a structure with in-plane anisotropy yields a two-lobe FFT image [22]. As can be seen, the inset FFT images in Fig. 3 are all two-lobe appearance, indicating that TiO_2 thin films deposited by GLAD technique are anisotropic structure.

The transmittance spectra of GLAD TiO_2 films are shown in Fig. 4. For thin films with given thickness, due to the interference of the incident light, constructive wave interference and destructive wave interference occur periodically. Therefore, the transmittance spectra of TiO_2 films exhibited many peaks and valleys. It can be seen that transmittance increases with the increase of incident angle. The effective refractive indices of GLAD TiO_2 films were calculated by Swanepoel's method [12,13]. These scattered refractive index were then fitted by Cauchy dispersion equation: $n(\lambda) = A_1 + A_2/\lambda^2 + A_3/\lambda^4$, as illustrated in Fig. 5. The effective refractive index of TiO_2 films decreases with the increase of flux incident angle. At wavelength $\lambda = 550$ nm, the effective refractive index changes from 2.18 to 1.60, which is less than that of the bulk materials ($n = 2.3$).

Base on the Bruggeman effective-medium approximation [23], the relationship between packing density and effective refractive index of GLAD TiO_2 film can be obtained, as shown in Table 1. The packing density of TiO_2 films decreases with the increase of incident angle. When the incoming atoms arrive at the substrate surface normally, TiO_2 films are compact, and the packing density is close to 1. At the flux angle of $\alpha = 75^\circ$, the packing density decrease to 0.493. The decrease of the refractive index and packing density in GLAD TiO_2 film can be ascribed to the porous structure in SEM images. By adjusting the flux incident angle, the effective refractive index and packing density of GLAD films can be engineered in a continuous range of values. One might also combine the microstructure evolution with the tailorable refractive index to produce refractive index gradient materials or other new optical coatings.

The anisotropic TiO_2 films with highly orientated columnar structure will result in optical birefringence. When transmittance spectra were measured with two orthogonal directions of incident polarized light, in-plane birefringence is defined as the difference between two in-plane refractive indices [22]. Fig. 6 illustrates the in-plane birefringence Δn for GLAD TiO_2 films. The in-plane birefringence Δn increases with the increase of flux incident angle. At $\alpha = 65^\circ$, birefringence reaches its maximum of $\Delta n = 0.067$. Higher flux angle would lead to the slight decrease of birefringence. For GLAD films, the characteristic packing density of the columns was the primary factor influencing the birefringence Δn, with column orientation playing a secondary role [24]. There is a critical packing density for the

Table 1
The packing density and effective refractive index of GLAD TiO_2 films

	Flux angle (°)						
	0	20	40	60	65	70	75
Refractive index	2.18	2.15	2.04	1.88	1.75	1.63	1.60
Packing density	0.908	0.885	0.804	0.689	0.597	0.514	0.493

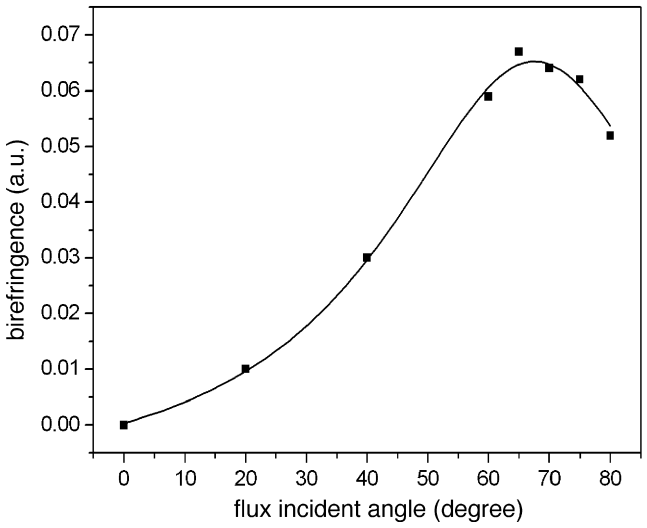

Fig. 6. The birefringence of GLAD TiO_2 films at different flux angles.

maximum value of birefringence [25]. Combining with Table 1, we can deduce that the critical packing density for GLAD TiO_2 films is about 0.597. The maximum birefringence of GLAD TiO_2 films is higher than that of the common bulk materials quartz ($\Delta n = 0.009$) and MgF_2 ($\Delta n = 0.012$) [22]. It is suggested that glancing angle deposition may offer an effective method to obtain the larger birefringence, and it seems particularly flexible to create designed devices such as retardation plate and polarizer.

4. Conclusion

TiO_2 films deposited by electron beam evaporation with glancing angle deposition exhibit highly orientated nanostructure composed of slanted columns. GLAD TiO_2 films are anisotropy, with the long axis parallel to the columnar growth direction. Column angle increases with the increase of flux angle. The slight deviation between the experimental and estimated column angle is related to the great surface curvature of nanostructured films. Due to the shadowing effect, the porous structure was obtained. Greater flux angles provide higher porosity. The effective refractive index decreases from 2.18 to 1.60 as flux angle increases from 0° to 75°. The birefringence varies as a function of the flux angle, with a maximum at approximately $\alpha = 65°$. Glancing angle deposition technique is an effective method to obtain the larger birefringence, which seems useful to create some devices such as retardation plate and polarizer.

References

[1] K. Robbie, M.J. Brett, J. Vac. Sci. Technol. A 15 (1997) 1460.
[2] A.C. Popta, M.M. Hawkeye, J.C. Sit, M.J. Brett, Opt. Lett. 29 (2004) 2545.
[3] T. Karabacak, J.P. Singh, Y.P. Zhao, G.C. Wang, T.M. Lu, Phys. Rev. B 68 (2003) 125408.
[4] K. Robbie, G. Beydaghyan, T. Brown, Rev. Sci. Instrum. 75 (2004) 1089.
[5] B. Dick, M.J. Brett, T. Smy, J. Vac. Sci. Technol. B 21 (2003) 23.
[6] K. Robbie, M.J. Brett, J. Vac. Sci. Technol. A 13 (1995) 2991.
[7] A. Goossens, E.L. Maloney, J. Schoonman, Chem. Vapor Depos. 43 (1998) 109.
[8] M.K. Kennedy, F.E. Kruis, H. Fissan, B.R. Mehta, G. Dumpich, J. Appl. Phys. 93 (2003) 551.
[9] N. Xu, Z. Shi, Y. Fan, J. Dong, J. Shi, M.Z.C. Hu, Ind. Eng. Chem. Res. 38 (1999) 373.
[10] B.S. Richards, J.E. Cotter, S.R. Wenham, Proceedings of the 28th IEEE PVSC, IEEE, USA, 2000, p. 375.
[11] A. Dakka, J. Lafait, C. Sella, S. Berthier, J.C. Martin, M. Maaza, Appl. Opt. 39 (2000) 2745.
[12] R. Swanepoel, J. Phys. E: Sci. Instrum. 16 (1983) 1214.
[13] S.Z. Shang, K. Yi, Z.X. Fan, J.D. Shao, Appl. Surf. Sci. 242 (2005) 437.
[14] B.A. Movchan, A.V. Demchishin, Phys. Met. Metallogr. 28 (1969) 83.
[15] M. Levichkova, V. Mankov, B. Mednikarov, K. Starbova, Surf. Coat. Tech. 141 (2001) 70.
[16] V.H. Kranenburg, C. Lodder, Mater. Sci. Eng. R 11 (1994) 295.
[17] D. Brian, B.J. Michael, Encyclopedia Nanosci. Nanotechnol. 6 (2004) 703.
[18] R. Messier, V.C. Venugopal, P.D. Sunal, J. Vac. Sci. Technol. A 18 (2000) 1538.
[19] J.M. Nieuwenhizen, H.B. Haanstra, Philips Tech. Rev. 27 (1966) 87.
[20] R.N. Tait, T. Smy, M.J. Brett, Thin Solid Films 226 (1993) 196.
[21] D. Vick, L.J. Friedrich, M.J. Brett, K. Robbie, M. Seto, T. Smy, Thin Solid Films 339 (1999) 88.
[22] G. Beydaghyan, K. Kaminska, T. Brown, K. Robbie, Appl. Optic. 43 (2004) 5343.
[23] D. Stroud, Superlattices Microst. 23 (1998) 567.
[24] T. Motohiro, Y. Taga, Appl. Optics 28 (1989) 2466.
[25] J.G. Wang, J.D. Shao, Z.X. Fan, Opt. Commun. 247 (2005) 107.